A R C H I V E S O F M E T A L L U R G Y A N D M A T E R I A L S
Volume 53 2008 Issue 1

W. RATUSZEK*, J. KOWALSKA*, J. RYŚ*, M. RUMIŃSKI*

THE EFFECT OF ($\gamma \rightarrow \alpha'$) PHASE TRANSFORMATION ON TEXTURE DEVELOPMENT IN METASTABLE AUSTENITIC STEEL

WPŁYW PRZEMIANY FAZOWEJ ($\gamma \rightarrow \alpha'$) NA ROZWÓJ TEKSTURY W METASTABILNEJ STALI AUSTENITYCZNEJ

The present research concerns the analysis of texture development in austenitic stainless steel AISI 301 subjected to cold-rolling at room temperature. X-ray phase analysis and magnetic investigations revealed the appearance of the α'-martensite within the structure of the steel after deformation. The volume fraction of strain induced martensite increased with increasing rolling reduction. The texture measurements of both phases were conducted from the centre layers of the rolled strip after selected thickness reductions.

Texture development in the case of steel AISI 301 was very complex since three processes proceeded simultaneously in the course of rolling, i.e. plastic deformation of the austenitic γ-phase, strain induced phase transformation ($\gamma \rightarrow \alpha'$) and deformation of the formed α'-martensite. The resultant deformation texture of the steel is described by the components from the textures of both phases, i.e. austenite and martensite. The rolling texture of austenite describe mainly orientations from the fibre α = <110>||ND and the major components of the martensite deformation texture are orientations from the fibres α_1 = <110>||RD and γ = <111>||ND. Transformations of the ideal orientations of austenite and transformations of the martensite texture ($\alpha' \rightarrow \gamma^T$) indicate that the martensitic transformation proceeded preferentially according to K u r d j u m o v-S a c h s (K-S) and N i s h i y a m a-W a s s e r m a n n (N-W) orientation relationships with variant selection.

Keywords: austenitic steel, deformation texture, phase transformation, strain induced martensite

Prezentowane badania dotyczą analizy rozwoju tekstury w austenitycznej stali nierdzewnej AISI 301 poddanej walcowaniu na zimno w temperaturze pokojowej. Dyfrakcyjna analiza fazowa i badania magnetyczne wykazały obecność martenzytu α' w strukturze stali po odkształceniu. Udział objętościowy martenzytu wzrastał ze stopniem odkształcenia. Pomiary tekstury obu faz przeprowadzono w warstwach środkowych walcowanych taśm po wybranych stopniach odkształcenia.

Rozwój tekstury odkształcenia w stali AISI 301 jest złożony gdyż podczas walcowania zachodzą równocześnie trzy procesy, tj.: odkształcenie plastyczne austenitu, przemiana fazowa ($\gamma \rightarrow \alpha'$) indukowana odkształceniem oraz odkształcenie powstałego martenzytu α'. Teksturę odkształcenia stali stanowią zatem składowe występujące zarówno w teksturze austenitu jak i w teksturze martenzytu. Teksturę walcowania austenitu opisują zasadniczo orientacje wchodzące w skład włókna α = <110>||KN, natomiast główne składowe tekstury martenzytu stanowią orientacje z włókien α_1 = <110>||KW oraz γ = <111>||KN. Transformacje idealnych orientacji austenitu oraz transformacje tekstury martenzytu ($\alpha' \rightarrow \gamma^T$) wskazują na to, że przemiana martenzytyczna zachodzi w sposób uprzywilejowany zgodnie z relacjami K u r d j u m o v a-S a c h s a (K-S) i N i s h i y a m y-W a s s e r m a n n a (N-W) z preferencyjnym wyborem określonych wariantów.

1. Introduction

Austenitic stainless steels are one of the most important groups of corrosion resistant metallic materials, with production estimated at about 2/3 of the total production of stainless steels. The austenitic grades usually contain a maximum of about 0.1% carbon, a minimum of 16% chromium and sufficient amount of nickel and/or manganese to retain an austenitic structure at all temperatures. However the chemical compositions of the 300 series of austenitic stainless steels do not always ensure the stability of the austenitic structure in the course of deformation, which sometimes undergo a strain-induced martensitic transformation [1–6]. The austenitic γ-phase may transform either to the α'-phase of body centred cubic ferrite or to the hexagonal ε-phase. The most often occurring ($\gamma \rightarrow \alpha'$) transformation leads to the formation of martensite within the austenite matrix. The strain induced transformation starts usually at much higher temperature (M_D) in comparison to the so-called martensite start temperature (M_S) upon cooling [1, 2, 7]. The amount of the martensite formed in the course of defor-

* DEPARTMENT OF PHYSICAL AND POWDER METALLURGY, AGH – UNIVERSITY OF SCIENCE AND TECHNOLOGY, 30-059 KRAKÓW, AV. MICKIEWICZA 30, POLAND

mation depends first of all on the chemical composition as well as deformation conditions, i.e. applied strain, temperature, etc. [1, 7, 8].

Increasing functional requirements imposed on structural materials designed for complex constructional and environmental applications led to the increase of importance of the texture developed upon their working. This especially applies to different grades of stainless steels.

Since cold-working is usually one of the final manufacturing steps and practically the only way to improve the strength of the austenitic stainless steels, it is very important to determine the mechanisms of plastic deformation in that case. An increase of strength of metastable austenitic steels in the course of deformation results not only from the strain hardening of the austenitic γ-phase but is also the effect of the formation of strain-induced α′-martensite. Both phases are plastically deformed and develop deformation textures, which additionally affect the mechanical behaviour, formability as well as the final properties of the steels [9–15]. That is why the object of the present research was the metastable austenitic steel AISI 301 subjected to cold-rolling within the wide range of deformations, which undergoes the martensitic transformation in the course of deformation. The main purpose of the investigations was to estimate the contribution of the ($\gamma \rightarrow \alpha'$) phase transformation, analysis of the texture development of austenite and martensite and determination of the crystallographic relations between both component phases.

2. Material and experimental procedure

The material examined in the present research was the austenitic stainless steel AISI 301 with the chemical composition given in Table 1. The steel was received in the form of strip after industrial thermo-mechanical pre-treatment and subsequently subjected to cold-rolling at room temperature up to 88% of thickness reduction.

TABLE 1
The chemical composition of the AISI 301 steel under examination (in weight %)

C	Cr	Ni	Mn	Mo	Si	Cu	Ti	Nb	N_2	Fe
0.1	17.6	7.48	1.08	0.114	0.6	0.14	<0.005	<0.005	0.077	balance

Based on the chemical composition of the AISI 301 steel the values of the following parameters were evaluated, namely; the stacking fault energy of the austenitic γ-phase SFE = 10.21 mJ/m^2, the martensite start temperature M_S = −131°C and the temperature of strain induced martensitic transformation $M_{D30/50}$ = 8°C.

The magnetic investigations were performed after the selected rolling reductions to determine the amount of the strain-induced martensitic α'-phase and the results are presented in Table 2.

TABLE 2
The amounts of strain-induced α'-martensite after the selected rolling reductions

$\varepsilon = \Delta h/h_0$ [%]	0	20	27	47	70	82	86	88
V_V^{α} [%]	0	12.2	23.2	38.5	69.3	77	77.7	86.6

X-ray investigations were conducted by means of Bruker diffractometer D8 Advance, using Co Kα radiation ($\lambda_{K\alpha}$ = 0.179 nm). X-ray examination included the phase analysis and the texture measurements from the centre layers of the rolled strip, for the initial state and after selected rolling reductions (Figs. 1 and 2). Texture analysis was performed on the basis of the orientation distribution functions (ODFs) calculated from the experimental pole figures. The incomplete pole figures were recorded of three planes for each of the component phase, i.e. the {111}, {200} and {220} planes for austenite and the {110}, {100} and {211} planes for the α′-martensite. The values of the orientation distribution functions f(g) along the typical orientation fibres were examined, i.e. α = <110>||ND, η = <001>||RD, τ = <110>||TD for the γ-phase and α_1 = <110>||RD, γ = <111>||ND, ε = <001>||ND for the α′-phase (Fig. 3). Additionally simulated transformations ($\alpha' \rightarrow \gamma^T$) of the martensite texture (experimental ODFs) were carried out according to selected preferential orientation relationships as well as transformations of the ideal orientations from the austenite rolling texture (Figs. 4 and 5).

The microstructure observations were carried out by means of the optical microscope Leica 3000N and the transmission electron microscope JEM 200MX from the longitudinal (ND-RD) sections of the rolled strip (Figs. 6–9).

3. Results and discussion

The X-ray phase analysis, the microstructure observations and the magnetic investigations revealed that the initial structure of AISI 301 steel, that is in as received state, is purely austenitic (Figs. 1, 6a, Table 2). The picks from the α′-martensite started to appear on diffraction patterns from the beginning of deformation process, simultaneously a decay of certain picks from austenite was observed as a result of the proceeding ($\gamma \rightarrow \alpha'$) phase transformation. After 20% of rolling reduction the 110α and 200α picks from martensite were weak as yet,

however with increasing deformation degree their intensity gradually increased. The next 211α pick from the α′-martensite appeared already after 27% of reduction (Fig. 1). It should be noted simultaneously that starting from the 20% of deformation the results of the phase analysis do not indicate at any significant contribution of the γ → ε transformation into the formation of the α′-martensite.

In the as received state the AISI 301 austenitic steel exhibited almost random initial orientation (Fig. 2). However austenite of the examined steel is the metastable phase and a development of deformation texture occurred very complex. In the course of cold-rolling the

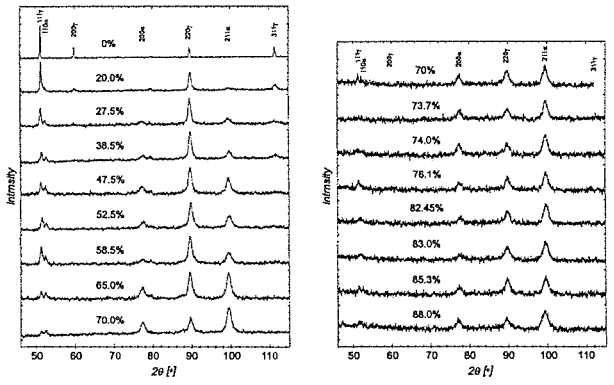

Fig. 1. X-ray diffraction patterns from the centre layers of the strip for the initial state and after selected rolling reductions

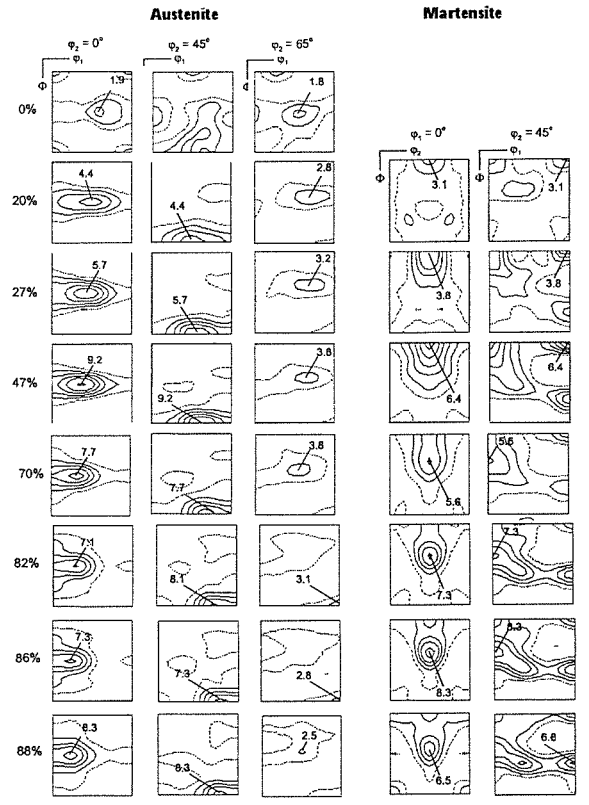

Fig. 2. Orientation distribution functions (ODFs) in sections $\varphi_2 = 0°$, $\varphi_2 = 45°$, $\varphi_2 = 65°$ for austenite and $\varphi_1 = 0°$, $\varphi_2 = 45°$ for martensite for the initial state and after selected rolling reductions

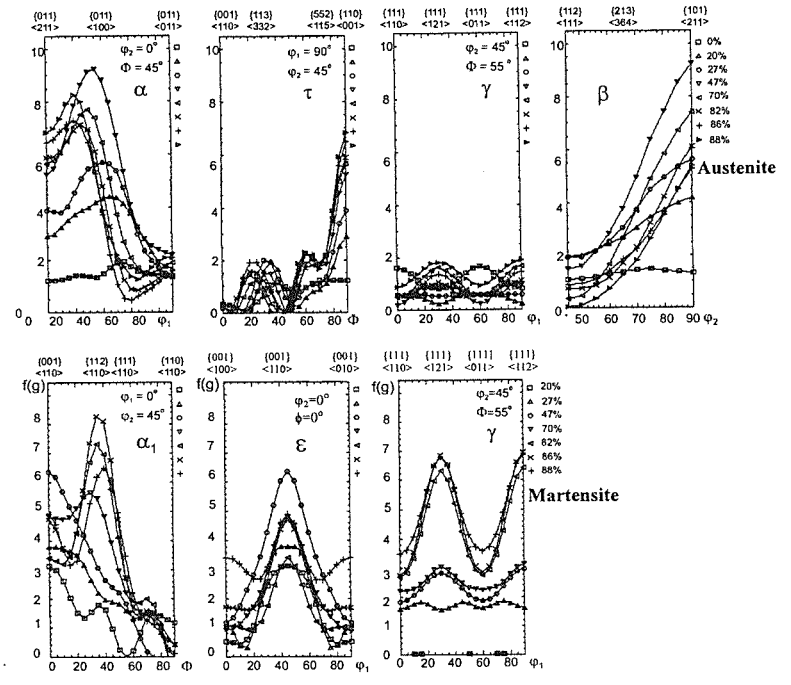

Fig. 3. Values of the orientation distribution functions f (g) along the orientation fibres α = <110>||ND, τ = <110>||TD δ = <111>||ND and β, for the γ-phase and α_1 = <110>||RD, ε = <001>||ND, γ = <111>||ND for the α′-phase after selected rolling reductions

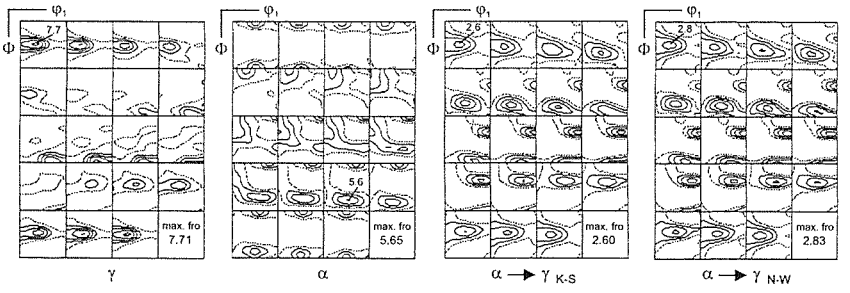

Fig. 4. Experimental ODFs for austenite and martensite and simulated transformations ($\alpha' \rightarrow \gamma^T$) of the martensite texture according to (K-S) and (N-W) orientation relationships in sections φ_2 =const

three processes proceeded simultaneously, namely; plastic deformation of the austenitic γ-phase, strain induced ($\gamma \rightarrow \alpha'$) martensitic transformation and deformation of previously formed α′-martensite. These processes resulted in the appearance of two phases in the structure of the steel with a definite crystallographic relationship and the orientation changes of both phases with increasing deformation. That is why the deformation texture of the examined metastable steel is described by the austenite and martensite texture components (Figs. 2 and 3).

The deformed austenite exhibited the fibrous texture, described by the following orientation fibers; α = <110>||ND, τ = <110>||TD, β ({110}<112>÷{123}<634>÷{112}<111>) and γ = <111>||ND. With increasing deformation degree the increase of the intensity of austenite texture was observed. The dominating components of the austenite texture occurred the orientations from the α = <110>||ND fiber, mainly the {110}<100> Goss orientation and the {110}<112> alloy-type component. However above 47% of rolling reduction the {110}<112> orientation is strongly weakened due to the ($\gamma \rightarrow \alpha'$) phase transformation. At the early stages of deformation the Cu-type {112}<111> orientation appeared additionally within the austenite texture and decayed at higher deformations (after 47% reduction). The appearance of the {111}<uvw> component in the austenite texture evidences a certain contribution of mechanical twinning in the texture formation (Figs. 2 and 3). In general the deformation texture of austenite is a typical texture of low stacking fault energy (SFE) material.

In the case of martensite the texture formation is more complex since it comprises the texture components from the newly formed martensite at a given deformation stage as well as components from previously formed and already deformed martensite. The continuous increase of texture intensity with increasing deformation degree is observed in the case of the α′-martensite. The dominating components within the texture of martensite after 70% of deformation are orientations from the fibres α_1 = <110>||RD, γ = <111>||ND and ε = <001>||ND (Figs. 2 and 3).

Transformations of the ideal orientations from the austenite texture ($\gamma \rightarrow \alpha'$) and transformations of the experimental orientation distribution functions (ODFs) of martensite ($\alpha' \rightarrow \gamma^T$) were conducted according to Kurdjumov-Sachs (K-S) and Nishiyama-Wassermann (N-W) relationships to verify the crystallographic relations between the major components of austenite and martensite textures (Figs. 4, 5). The comparison of the austenite ODFs after deformation with those after ($\alpha' \rightarrow \gamma^T$) transformation indicates that K-S and N-W orientation relationships describe very well the crystallographic relations between both phases . It should be noted however that the transformations were performed without taking into account the variant selection hence the lower maximum values of the resultant ODFs. Differences between austenite ODFs after deformation and after ($\alpha' \rightarrow \gamma^T$) transformation result first of all from the fact that the martensite ODF subjected to transformation comprises texture components of martensite formed at a given deformation stage and previously formed martensite deformed in the course of rolling (Fig. 4).

Texture analysis and simulated transformations indicate at the fact that crystallographic relations between the major components of the austenite and martensite textures are best described by Kurdjumov-Sachs (K-S) orientation relation (Fig. 5a). For example with increasing deformation degree the enhanced intensity of the {111}<112> component of the martensite texture was observed with simultaneous decrease in the intensity of the {110}<112> orientation from the austenite texture. The absence of the {112}<111> and {123}<111> orientations within the deformation texture of austenite and their appearance in simulated ODFs obtained through the ($\alpha' \rightarrow \gamma^T$) transformation of martensite texture indicates that the martensite was formed from austenite grains with these orientations. The {112}<110> orientation of martensite was transformed from the {112}<111> austenite texture component according to K-S orientation relationship. Similarly the major austenite texture components transform into the following orientations from the martensite texture through the K-S relation: {110}<001>γ →{332}<110>α,

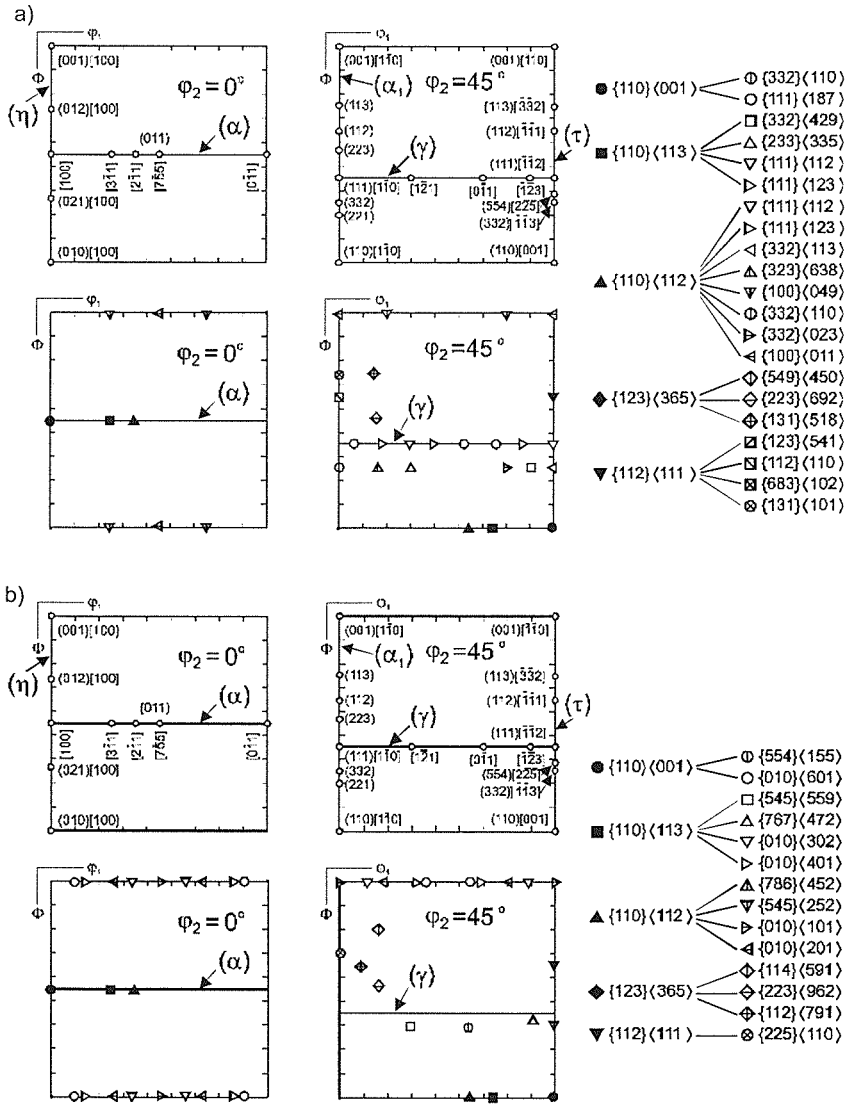

Fig. 5. The orientation fibres from the austenite and martensite textures and the crystallographic relations between the selected ideal orientations described by Kurdjumov-Sachs (K-S) and Nishiyama-Wasserman (N-W) relationships (a, b – respectively)

{110}<113>γ →{111}<112>α, {110}<112>γ →{332}<110>α, {110}<112>γ →{100}<011> (Fig. 5a). On the other hand the N i s h i y a m a-W a s s e r m a n (N-W) relationship gives equally well description of the orientation relation between the textures of both phases as a whole (Figs. 4 and 5b).

Within the microstructure of AISI 301 steel in the as received (initial) state the equiaxed austenite grains and annealing twins are observed (Fig. 6a). After 27% of rolling reduction the effects of strain localization were revealed in some grains, which occurred the preferential places for the formation of the α′-martensite (Fig. 6b). With increasing deformation degree an increase of banding of the austenite-martensite two-phase structure is observed. After 70% of reduction the bands of both phases were arranged nearly parallel to the rolling plane and displayed corrugated shapes resulting from strain localization proceeding at higher strains (Fig. 6c). The microstructure analysis conducted by means of transmission electron microscopy confirmed the fact that formation of the α′-martensite proceeds within areas the high dislocation density in the austenite matrix (Fig. 7a). Dark field image from the 200_γ diffraction spot displays the arrangement of both phases within the microstructure (Fig. 7b). Selected area electron diffractions (SAED) from the three marked areas in figure 7a indicate at the essentially the same type of the crystallographic relation between the austenite matrix and the formed α′-phase, that is, the K-S $[011]_\gamma \| [\bar{1}11]_\alpha$ relationship. The microstructures after 70% of reduction (Fig. 8) from the

Fig. 6. Microstructures of AISI 301 steel for the initial state (a) and after 27.5% (b) and 70% of rolling reduction (c); the (ND-RD) longitudinal sections of the rolled strip

longitudinal (ND-RD) section of the strip and after 88% of deformation (Fig. 9) as observed parallel to the rolling plane indicate at the formation of the fine-grained microstructure with high dislocation density. The character of both diffraction patterns, with a significant spread (extension) of diffraction spots, confirms the fact that the microstructure comprises the mixture of two strongly deformed phases, that is the austenitic γ- phase and the α′-martensite (Figs. 8 and 9). The magnetic investigations revealed 86.6% of the martensite volume fraction within the structure of the steel after 88% of deformation. Simultaneously the microstructure at this deformation level displays very high dislocation density on the background of the martensite laths. These results are in agreement with the investigations of the metastable austenitic steel by Takaki et al [15], where the ($\gamma \rightarrow \alpha'$) transformation led to the complete transition of austenite and further deformation proceeded by deformation of martensite laths resulting in formation of highly dislocated cell structure. That is why it may be concluded that deformation of the metastable austenitic steel AISI 301 comprised of three processes, i.e. deformation of the austenitic γ-phase, the strain induced martensitic transformation ($\gamma \rightarrow \alpha'$) and deformation of previously formed α′-martensite. All these processes contributed to the formation of the resultant texture, which included deformation texture components from both phases.

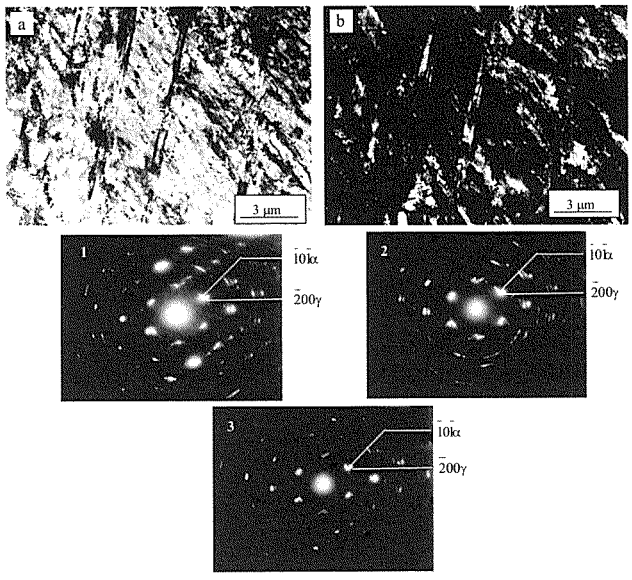

Fig. 7. Microstructure of the AISI 301 steel after 70% of rolling reduction from the layer parallel to the rolling plane; TEM bright field image (a) and dark field image - 200γ (b) – electron diffraction patterns from the marked areas

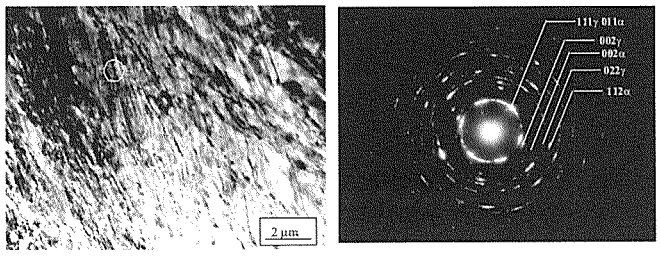

Fig. 8. Microstructure of the AISI 301 steel after 70% of rolling reduction from the longitudinal (ND-RD) section – electron diffraction pattern from the marked area

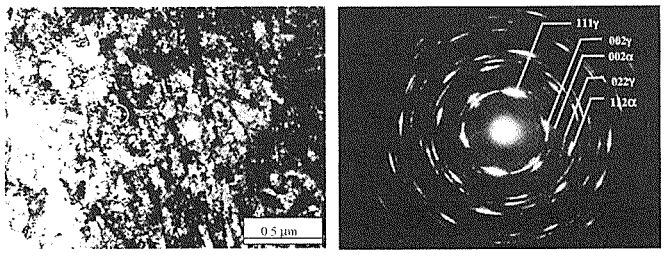

Fig. 9. Microstructure of the AISI 301 steel after 88% of rolling reduction from the layer parallel to the rolling plane – electron diffraction pattern from the marked area

4. Concluding remarks

1. The examined AISI 301 stainless steel grade is the metastable austenitic steel since plastic deformation induces the martensitic phase transformation ($\gamma \rightarrow \alpha'$) within the whole range of applied strains.
2. Texture development in AISI 301 steel is rather complex because the following phenomena take place in the course of plastic working: deformation of the austenitic γ-phase, strain induced phase transformation ($\gamma \rightarrow \alpha'$) and deformation of the previously formed α′-martensite.
3. The dominant components of the austenite deformation texture are the orientations from the α =<110>||ND fibre and the -phase tends to develop the alloy type {110}<112> final texture, typical for low stacking fault energy (SFE) alloys.
4. Continuous development of the texture of martensite formed upon deformation is observed, which evolves towards the texture characteristic for deformed ferrite, i.e. the texture with orientation components of the <110>||RD type.
5. Crystallographic relations between the textures of the austenitic γ-phase and the α′-martensite formed upon deformation are best described by the Kurdjumov-Sachs (K-S) as well as by the Nishiyama-Wasserman (N-W) relationships.
6. Simulated transformations of the experimental and ideal ODFs indicate that the variant selection takes place in the course of transformation and not all of the variants (K-S / 24 and N-W / 12) are equally probable.

Acknowledgements

The work was supported by the Polish Committee for Scientific Research (KBN) under the contract No. 4.T08B.029.25.

REFERENCES

[1] T. Angel, Formation of Martensite in Austenitic Stainless Steels Effect of Deformation, Temperature and Composition, Journal of the Iron and Steel Institute (1954), 165-174.

[2] A. F. Padilha, R. L. Plaut, P. R. Rios, Annealing of Cold-Worked Austenitic Stainless, ISIJ International **43**, 135-143 (2003).

[3] A. F. Padilha, P. R. Rios, Decomposition of Austenite in Austenitic Stainless Steels, ISIJ International **42**, 325-337 (2002).

[4] S. Ganesh Sundara Raman, K. A. Padmanabhan, Tensile Deformation-Induced Martensitic Transformation in AISI 304LN Austenitic Stainless Steel, Journal of Materials Science Letters **13**, 389-392 (1994).

[5] L. Mangonon, G. Thomas, Structure and Properties of Thermal-Mechanically Treated 304 Stainless Steel, Metallurgical Transactions **1**, 1587-1594 (1970).

[6] L. Mangonon, G. Thomas, The Martensite Phase in 304 Stainless Steel, Metallurgical Transactions **1**, 1577-1586 (1970).

[7] P. Lacombe, G. Béranger, Les editions de physique, France 1993.

[8] H. Fujita, S. Ueda, Stacking Faults and FCC (γ)→HCP (ε) Transformation in 18/8-Type Stainless Steel, Acta Metallurgica **20**, 759-767 (1972).

[9] J. Łuksza, M. Rumiński, W. Ratuszek, M. Blicharski, Texture evolution and variations of α-phase volume fraction in cold-rolled AISI 301 steel strip, Journal of Materials Processing Technology **177**, 555-560 (2006).

[10] A. M. Lopez, C. S. Da Costa Viana, A Discrete Orientation Model for the FCC-to-BCC Phase Transformation, ICOTOM **12**, 322-327 (1999).

[11] W. Ratuszek, W. Kowalska, M. Rumiński, K. Chruściel, Rozwój tekstury podczas walcowania na zimno austenitycznej stali AISI 301, Problemy współcz. techniki w aspekcie inżynierii i edukacji (2005), 69-74.

[12] B. Ravi Kumar, A. K. Singh, S. Das, D. K. Bhattacharya, Cold Rolling in AISI 304 Stainless Steel, Materials Science and Engineering **A364**, 132-139 (2004).

[13] D. Raabe, Texture and Microstructure Evolution During Cold Rolling of a Strip Cast and of Hot Rolled Austenitic Stainless Steel, Acta Materialia **45**, 3, 1137-1151 (1997).

[14] C. Herrera, R. L. Plaut, A. F. Padilha, Mikrostructural Refinement during Annealing of Plastically Deformed Austenitic Stainless Steels, Materials Science Forum **550**, 423-428 (2007).

[15] S. Takaki, K. Tomimura, S. Ueda, Effect of Pre-Cold-Working on Diffusional Reversion of Deformation in Metastable Austenitic Stainless Steel, ISIJ International **34**, 6, 522-527 (1994).

Received: 3 December 2007.